

## Electronic Supplementary Information

### Bicrystalline TiO<sub>2</sub> with Controllable Anatase/Brookite Phase Content for Enhanced CO<sub>2</sub> Photoreduction to Fuels

Huilei Zhao<sup>a</sup>, Lianjun Liu<sup>a</sup>, Jean M. Andino<sup>b,c</sup>, Ying Li<sup>a\*</sup>

<sup>a</sup> Mechanical Engineering Department, University of Wisconsin-Milwaukee

<sup>b</sup> Chemical Engineering and <sup>c</sup> Civil, Environmental, and Sustainable Engineering, Arizona State University

\* Corresponding Author: 3200 N Cramer St, Milwaukee, Wisconsin, U.S.A. Fax: (+1) 414-229-6958;

Tel: (+1) 414-229-3716; E-mail: liying@uwm.edu.

#### Rietveld Refinement of the XRD data

The Rietveld refinement method is a commonly used method to calculate the crystal phase content. Because the Rietveld method for quantitative phase analysis uses a whole pattern fitting, both lattice parameters and space group are used to constrain the peak positions, and peak intensities are constrained by crystal structure; hence, the Rietveld refinement is known for its greater accuracy than single peak fitting method.<sup>1-4</sup>

Figures S1-S4 show the Rietveld refinement fitting results for the four bicrystalline TiO<sub>2</sub> samples. It can be observed that all the black solid fitting lines of the Rietveld refinement match the experimental XRD data (blue dots) very well. The low fluctuation of the goodness of fitting (GOF) curve at the bottom indicates a high reliability of the Rietveld refinement method.

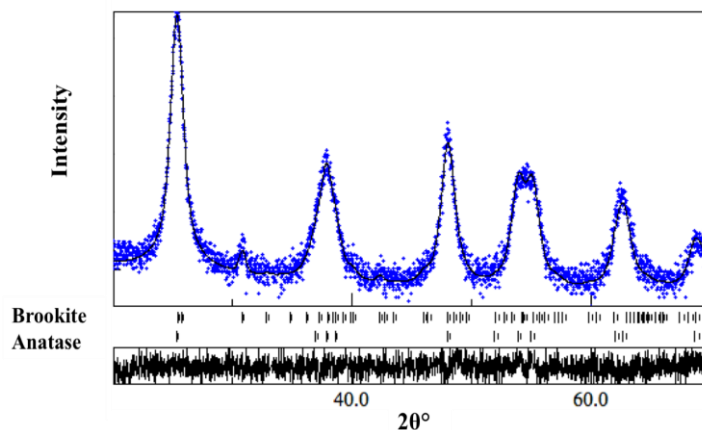


Figure S1. Rietveld refinement of the XRD data for the sample of A<sub>96</sub>B<sub>4</sub>

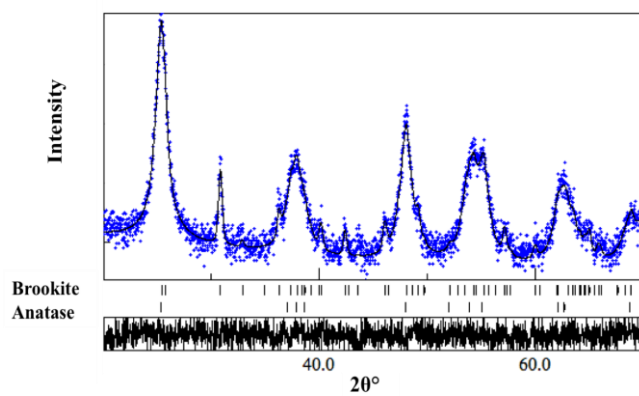


Figure S2. Rietveld refinement of the XRD data for the sample of  $A_{75}B_{25}$

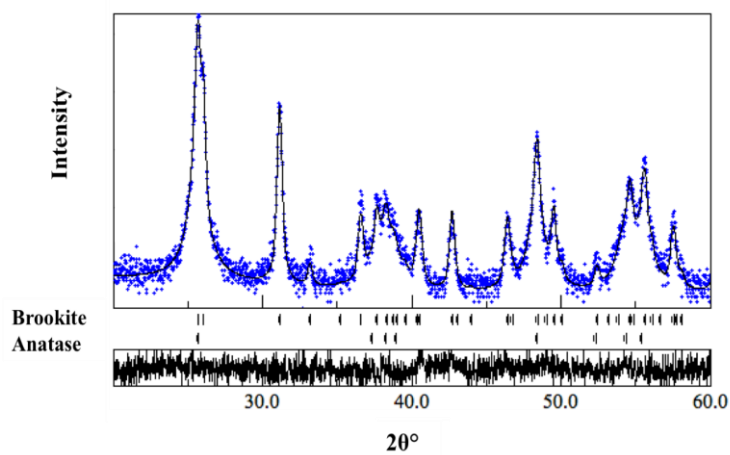


Figure S3. Rietveld refinement of the XRD data for the sample of  $A_{50}B_{50}$

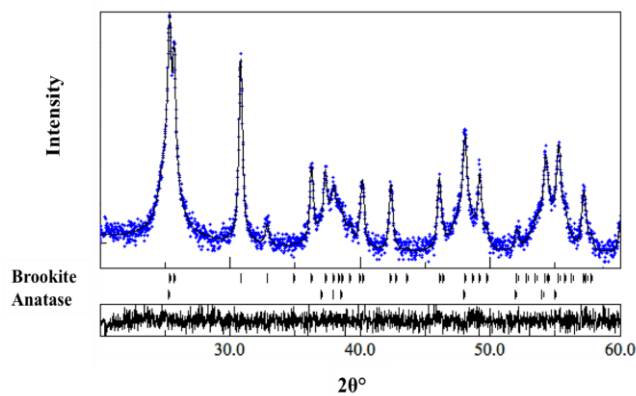
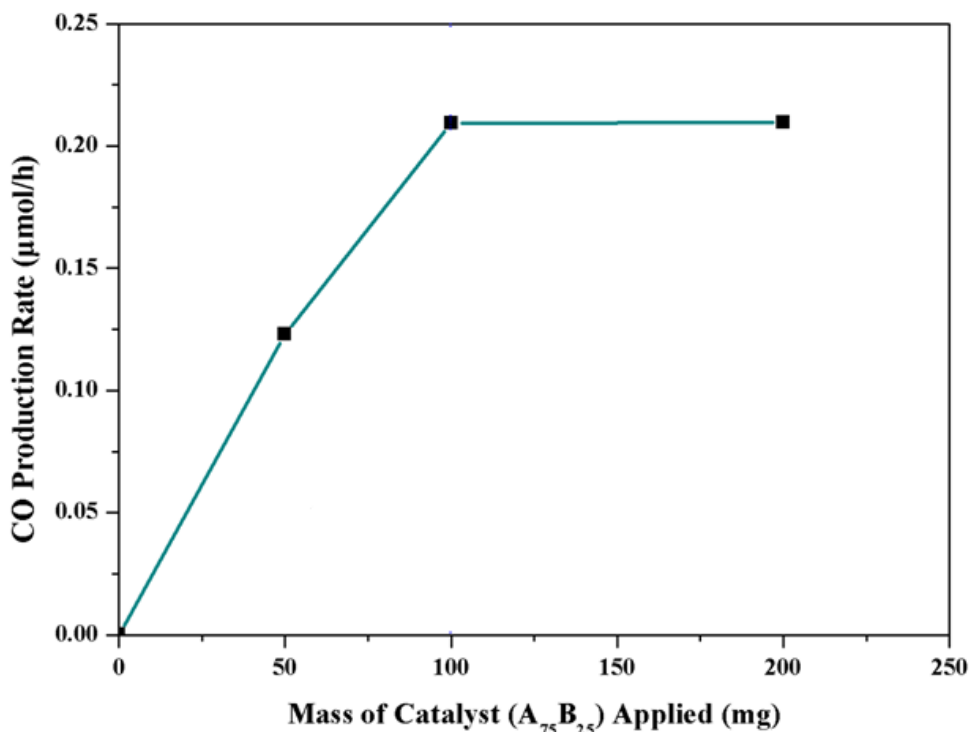


Figure S4. Rietveld refinement of the XRD data for the sample of  $A_{37}B_{63}$

### Effect of catalyst mass on the photocatalytic activity

To investigate the effect of catalyst mass, two additional experiments were carried out on the most active  $A_{75}B_{25}$ , i.e., reducing the amount of catalyst from 100 mg to 50 mg, and increasing to 200 mg. The activity measurement results are shown in Figure S5. When reducing the catalyst amount to 50 mg, the CO production rate was 0.12  $\mu\text{mol/h}$ , about 58% of that when using 100 mg (0.21  $\mu\text{mol/h}$ ). When increasing the catalyst amount of 200 mg, the CO production rate remained almost the same as that when using 100 mg (0.21  $\mu\text{mol/h}$ ). The catalytic activity vs. catalyst mass relation presented in Figure S5 matches the literature results on photocatalytic properties.<sup>5</sup> The most likely reason that further increasing the catalyst mass did not increase the catalytic activity is because 100 mg catalyst, which was well dispersed in the photoreactor, has already reached the maximum light absorption. Besides, the catalytic activity of 50 mg and 100 mg catalysts was almost linear with the mass. Hence, the amount used (100 mg) for all catalysts in this study was appropriate and representative of the intrinsic catalytic activity of the catalyst.



**Figure S5.** The CO production rate versus the mass of catalysts ( $A_{75}B_{25}$ ) applied in  $\text{CO}_2$  photoreduction experiments

### **Evidence of concurrent photoreduction (CO<sub>2</sub> reduction to CO and CH<sub>4</sub>) and photooxidation (H<sub>2</sub>O oxidation to O<sub>2</sub>)**

Figure S6 shows both the O<sub>2</sub>/N<sub>2</sub> ratio and the CO/CH<sub>4</sub> production rates as a function of time using the A<sub>75</sub>B<sub>25</sub> sample before, during and after the photo-illumination. Upon photo-illumination, the O<sub>2</sub>/N<sub>2</sub> ratio decreased in the first 60 min, and in the same time the CO/CH<sub>4</sub> production rates increased. The first 15 min showed the most dramatic changes for both the O<sub>2</sub>/N<sub>2</sub> ratio and the CO/CH<sub>4</sub> production. Because the photo-excited electrons are non-selective, they will react with any electron acceptors including both O<sub>2</sub> and CO<sub>2</sub>. The much higher CO<sub>2</sub> concentration (~97%) than O<sub>2</sub> (a few hundred ppm) in the reactor may help the kinetics of CO<sub>2</sub> reduction by electrons, although the electron scavenging ability of a single O<sub>2</sub> molecule may be stronger than a CO<sub>2</sub> molecule. Thus, it is reasonable that we see the decrease in the O<sub>2</sub>/N<sub>2</sub> ratio and the increase in the CO/CH<sub>4</sub> production in the same time. Since there are no other compounds in the reactor system that can directly react with O<sub>2</sub>, we believe the observed decrease in O<sub>2</sub> upon photo-illumination is indeed due to electron-scavenging effect:  $O_2 + e^- \rightarrow O_2^-$ . The gradual increase in the O<sub>2</sub>/N<sub>2</sub> ratio after 60 min photo-irradiation indicated the generation of O<sub>2</sub> through oxidation of H<sub>2</sub>O with photogenerated holes,  $H_2O + 2h^+ \rightarrow 2H^+ + (1/2) O_2$ . Because the increasing amount of generated O<sub>2</sub> outweighed the concurrent O<sub>2</sub> consumption process, the net result was that the O<sub>2</sub>/N<sub>2</sub> ratio gradually increased with time. The decreasing production rates of CO and CH<sub>4</sub> after 60 min photo-irradiation may be explained by the accumulation of non-reactive intermediates on the surface (see the in situ DRIFTS results in Section 3.4). The deactivation of the photocatalyst in CO<sub>2</sub> reduction around 240 min is also well correlated with the result that almost no significant O<sub>2</sub> was produced after 200 min. The above results demonstrate that both photoreduction (CO<sub>2</sub> reduction to CO and CH<sub>4</sub>) and photooxidation (H<sub>2</sub>O oxidation to O<sub>2</sub>) reactions occurred simultaneously in the reactor system.

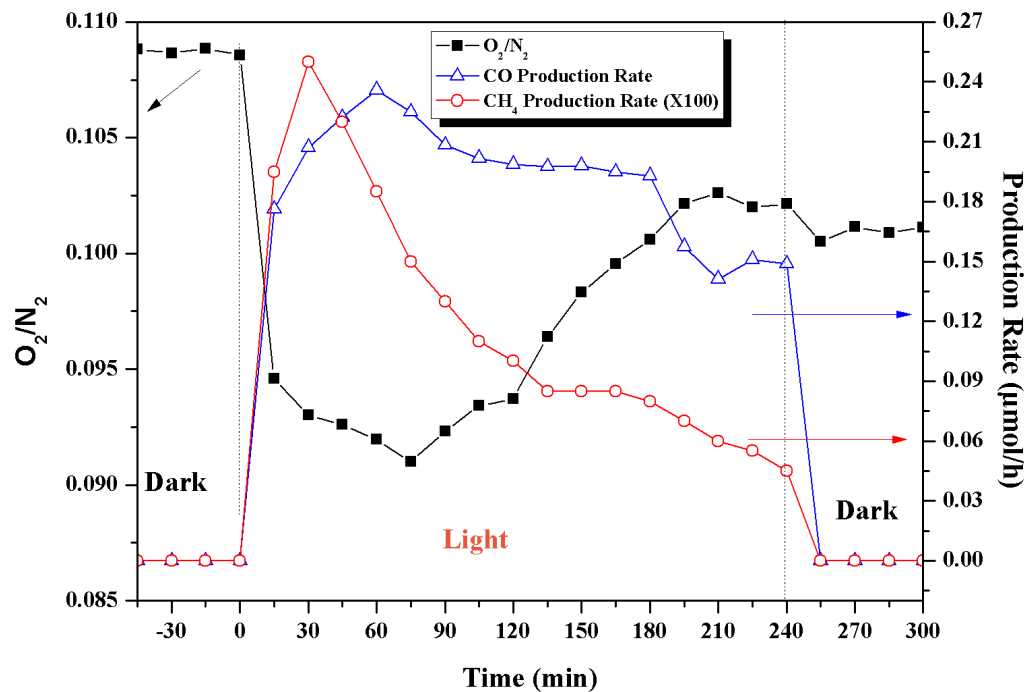


**Figure S6.** Time dependence of the volumetric ratio of O<sub>2</sub>/N<sub>2</sub> and the CO/CH<sub>4</sub> production rates before, during and after the photoreduction of CO<sub>2</sub> with H<sub>2</sub>O on the sample of A<sub>75</sub>B<sub>25</sub>.

## Reference

1. A. Z. Simoes, L. S. Cavalcante, F. Moura, E. Longo and J. A. Varela, *J Alloy Compd.*, 2011, **509**, 5326-5335.
2. Rashmi, N. Singh and A. K. Sarkar, *Powder Diffr.*, 2004, **19**, 141-144.
3. T. Balic-Zunic, *Powder Diffr.*, 2002, **17**, 287-289.
4. R. J. Hill and C. J. Howard, *J. Appl. Crystallogr.*, 1987, **20**, 467-474.
5. L. Davydov, S. E. Pratsinis and P. G. Smirniotis, *Environ. Sci. Technol.*, 2000, **34**, 3435-3442.